Decision Directed Autocorrelation Receivers for Pulsed Ultra-Wideband Systems

Shiwei Zhao, *Student Member, IEEE*, Huaping Liu, *Member, IEEE*, and Zhi Tian, *Member, IEEE*

***Abstract*— The need for effective capture of multipath energy presents a key challenge to receiver design for pulsed ultra-wideband (UWB) systems operating in non-line-of-sight propagation environments. Conventional RAKE receivers can capture only a fraction of the received signal energy under practical implementation constraints, and have to deal with stringent synchronization and channel estimation requirements. Transmit-reference and autocorrelation receivers can effectively collect energy from all the received multipath components without explicit channel estimation, but the detection performance is limited by noise enhancement effects and the data rate drops by 50% because of pilot symbol overhead. In this paper, we develop decision-directed autocorrelation (DDA) receivers for effective multipath energy capture at low complexity. Operating in an adaptive decision-directed mode, the proposed DDA methods can considerably lower the noise level in the self-derived template waveform, thus improving overall detection performance. There is little loss in energy efficiency since no reference pilots are required during adaptation. Analytical performance analysis along with corroborating simulations is performed to evaluate the error performance of the proposed receivers in indoor lognormal fading channels.**

***Index Terms*— Autocorrelation, decision direction, energy capture, hard decoding, soft decoding, transmit-reference, ultra wideband communications.**

I. Introduction

ULTRA-WIDEBAND (UWB) communications has emerged as a promising technology for short-range, high-speed wireless applications [1], [2]. With its enormous bandwidth, UWB signaling comes with uniquely attractive features that offer the potential for very high data rates over short distances (in the order of 10-20 meters). UWB radios operate at extremely low transmitted power density under FCC spectral regulations, which open up a host of new wireless services capable of overlay with legacy narrowband systems. By conveying information over ultra-short pulses, pulsed UWB radios also provide very fine temporal resolution, which may lead to high-performance detector design when ample multipath diversity can be properly collected.

Energy capture in the presence of multipath propagation is conventionally done by RAKE receivers [3], [4]. However, in a pulse-based UWB system, the number of resolvable paths could reach tens to over a hundred in typical indoor propagation environments [5], which imposes technical hurdles as well as implementation difficulties. In order to capture a considerable portion of the signal energy scattered in multipath components, a traditional RAKE-based digital receiver not only has to sample and operate at a minimum of hundreds of MHz to even multi-GHz clock rates, but also requires a very large number of RAKE fingers. Realizing optimal RAKE reception performance requires accurate channel and timing knowledge, which is quite challenging to obtain as the number of resolvable paths grows. Moreover, the received pulse shapes of resolvable multipath might be distorted differently due to diffraction, which makes it suboptimal to use line-of-sight signal waveform as the correlation template in RAKE reception. Because of these issues unique to UWB pulsed radios, the popular RAKE receiver design can be ineffective or impractical.

As a suboptimal, low-complexity alternative, transmit-reference (TR) or autocorrelation receivers [6] – [13] have been investigated, which offer better multipath capture capability at much lower hardware complexity than RAKE receivers. In the TR scheme [6], pulses are transmitted in pairs, where the first pulse of each pair serves as the reference signal and the second pulse is data modulated. In the receiver, the channel-inflicted reference signal is used as the template waveform to correlate with the ensuing waveform for symbol detection. In a slow fading environment, TR collects multipath energy efficiently without requiring multipath tracking or channel estimation. Analog autocorrelation also alleviates the burden on A-D converters, thus lowering the power consumption by interface circuits in the UWB regime. Nevertheless, TR autocorrelators entail several drawbacks: the use of reference pulses increases transmission overhead and reduces data rate, which results in reduced transmission power efficiency; the bit-error-rate (BER) performance is limited by the noise term in the reference signal [6], [7]. Different methods have been proposed to improve the error performance either by modulation parameter selection [8], signal set selection [9], or receiver processing [7], [10]–[13].

In this paper, we propose decision-directed autocorrelation (DDA) receivers that not only offer considerable performance improvement but also significantly reduce the signaling overhead (to zero asymptotically) compared with existing TR-type schemes. In DDA, a near-optimal correlation template is constructed directly from information-bearing received waveforms. Specifically, received symbol waveforms preceding the current symbol are delayed, multiplied by symbol decisions

Manuscript received September 23, 2004; revised March 26, 2005; accepted September 25, 2005. The associate editor coordinating the review of this paper and approving it for publication was X. Wang. Z. Tian was supported by the NSF Grant No. CCR-0238174. This work was presented in part at the IEEE RAWCON'2004, Atlanta, Sept. 2004.

S. Zhao and H. Liu are with the School of Electrical Engineering and Computer Science, Oregon State University, Corvallis, OR 97331 USA (e-mail: zhao@eecs.orst.edu; hliu@eecs.orst.edu).

Z. Tian is with the Department of Electrical and Computer Engineering Michigan Technological University, Houghton, MI 49931 USA (e-mail: ztian@mtu.edu).

Digital Object Identifier 10.1109/TWC.2006.04644

within the corresponding symbol window, and averaged to form the template waveform adaptively. This template is then used to correlate with the received signal to detect the current symbol. Because decision-directed (DD) symbol estimates are used in lieu of pilot symbols, the signaling overhead is reduced to zero asymptotically as the data length increases. Operating at the symbol rate, the DDA scheme does not require multipath tracking or channel estimation as is required in a RAKE receiver, and is still able to capture energy from all received multipath components. It offers considerable performance improvement over TR because noise in the self-derived template waveform is effectively alleviated through the decision-directed waveform averaging process. Provided that past symbol decisions are accurate, the resulting template is asymptotically optimal for correlation detection.

It is appropriate to compare the proposed DDA receiver with some existing schemes. In [7], [8], [10], the template waveform is formed by averaging over multiple previous reference pulses for autocorrelation operations. Unlike our scheme, these reference pulses result in signal power overheads and throughput penalties. In [12], a differential TR receiver was proposed to avoid reference pulses, but its error performance is limited by the noisy reference signal that is constructed without waveform averaging. The independent work [13] developed almost in parallel with this work [14] presented a decision-directed adaptive differential receiver, which is very similar to one of the recursive DDA detectors we will detail in Section III-B. The focus of this paper is to develop three different algorithms for obtaining the template waveforms based on the DDA principle. We not only establish the optimality of the three algorithms, but also compare their relative advantages and disadvantages. We also provide analytical error performance of these algorithms in practical lognormal fading environments.

This paper is organized as follows. In Section II, the signal model for UWB impulse radio is described. The DDA approach is presented in Section III, along with several adaptive design options. Based on practical indoor UWB channel environments, analytical performance evaluation follows in Section IV, which includes results that assess both error performance and convergence rate of DDA. Numerical results for indoor UWB channel environments are provided in Section V. Section VI presents a performance-enhancing strategy via soft decoding, followed by concluding remarks in Section VII. For clarity, this paper focuses on binary pulse amplitude modulation (PAM), while generalizations of the DDA approach to other modulation schemes are straightforward.

II. System and Channel Model

In binary PAM UWB signaling, information bits $b[i] \in \{1, -1\}$ are transmitted over a train of ultra-short pulses $p(t)$ of pulse width T_p. The bit interval T_b is much larger than T_p, resulting in a low duty cycle transmission form. With energy E_b per bit, the transmitted PAM UWB waveform is given by

$$s(t) = \sqrt{E_b} \sum_{i=-\infty}^{\infty} b[i]p(t - iT_b). \tag{1}$$

Pulsed UWB signaling gives rise to frequency selective channels, whose impulse responses can be modeled as tapped delay line filters. The aggregate channel after convolving with the transmitted pulse is given by [5]

$$h(t) = \sum_{l=0}^{L-1} \alpha_l p(t - \tau_l), \tag{2}$$

where L is the total number of multipath components, each with path fading gain α_l and delay τ_l relative to the first path. Perfect timing is assumed by setting $\tau_0 = 0$. The received waveform is thus given by

$$r(t) = \sum_{l=0}^{L-1} \alpha_l s(t-\tau_l) + n_o(t) = \sqrt{E_b} \sum_{i=-\infty}^{\infty} b[i]h(t-iT_b) + n_o(t), \tag{3}$$

where $n_o(t)$ is the ambient noise typically treated as a zero-mean white Gaussian process with power spectral density (PSD) $N_o/2$. To avoid channel-induced inter-symbol interference (ISI), the bit interval T_b is selected to be larger than the channel delay spread τ_{L-1}. In practice, the received signal $r(t)$ is first passed through an ideal bandpass filter with center frequency f_0 and double-sided bandwidth B which is chosen to be wide enough, larger than the signal's 10dB bandwidth, to avoid filter-induced ISI. It is also assumed that B is an integer multiple of $1/(2T_b)$. The filtered noise $n(t)$ is no longer white, but its autocorrelation in time can be very small due to the ultra-wide filter bandwidth B. The autocorrelation function of $n(t)$ is

$$R_n(\tau) = E\{n(t)n(t+\tau)\} = N_o B \frac{\sin(2\pi B\tau)}{2\pi B\tau} \cos(2\pi f_0 \tau). \tag{4}$$

Free of ISI, the received signal waveform can be described by the following one-shot model within each symbol period $t \in [iT_b, (i+1)T_b)$:

$$r_i(t) := r(t+iT_b) = \sqrt{E_b} b[i]h(t) + n_i(t), \qquad t \in [0, T_b) \tag{5}$$

where $n_i(t) := n(t + iT_b)$, $t \in [0, T_b)$, is the corresponding T_b-long segment of the filtered noise $n(t)$.

Although our detector design will not rely on any specific channel model, it is appropriate to examine the channel model measured by the IEEE 802.15.3a working group [5], which will be used in our performance analysis. In [5], the channel path gain α_l is modeled as $\alpha_l = \lambda_l \beta_l$, where $\lambda_l \in \{\pm 1\}$ with equal probability accounts for random pulse polarity inversion resulted from reflection. The path magnitude β_l is real-valued and follows a log-normal distribution for indoor UWB channels. The standard deviation of fading amplitudes across $\{\beta_l\}$ is typically in the range of $3 - 5$ dB. Because multipath components tend to arrive in clusters [5], τ_l in (2) can be expressed as $\tau_l = \mu_c + \nu_{m,c}$, where μ_c is the delay of the c^{th} cluster that the l^{th} path belongs to, and $\nu_{m,c}$ is the delay (relative to μ_c) of the m^{th} multipath component in the c^{th} cluster. The power delay profile of the channel is modeled as exponentially decaying by rays and clusters: the relative power of the l^{th} path to the first path can be expressed as $E\{|\alpha_l|^2\} = E\{|\alpha_0|^2\} e^{-\mu_c/\Gamma} e^{-\nu_m/\gamma}$, where Γ and γ are the decaying factors for the corresponding cluster and ray, respectively.

III. Decision Directed Autocorrelation Receivers

For symbol-by-symbol correlation-based detection, the optimal correlation template is given by the aggregate channel waveform $h(t)$. Focusing on the one-shot model in (5), we first examine the optimal channel estimate of $h(t)$ given $\{r_i(t)\}_{i=0}^{\infty}$. When $h(t)$ is treated as deterministic but unknown, the optimal minimum mean square estimator of $h(t)$ (notwithstanding a scaling factor $\sqrt{E_b}$) conditioned on real-valued $\mathbf{b} := \{b[i]\}$ can be formulated as $\hat{h}(t) = argmin_{h(t)} E\{|r_i(t) - b[i]h(t)|^2\}$, which leads to

$$\hat{h}(t) = E\left\{b^{-1}[i]r_i(t)\right\}. \tag{6}$$

When it comes to binary PAM, we may equivalently replace $b^{-1}[i]$ by $b[i]$ for convenience. This channel estimator makes intuitive sense, because multiplying each received symbol waveform by the corresponding symbol takes out the symbol effect but retains the channel information. The remaining question is: how can we find $\hat{h}(t)$ in the absence of the knowledge of $\mathbf{b}$?

Our approach towards practical realizations of (6) in a slowly fading environment (channel remains static over a large number of bit intervals) is to employ DD operations. To this end, we construct a finite-sample implementation of (6) at the k-th symbol period as follows:

$$\hat{h}_k(t) = \frac{1}{k}\sum_{i=0}^{k-1}\hat{b}[i]r_i(t), \tag{7}$$

where $\hat{b}[i]$ are symbol decisions made in the past, and $\hat{h}_k(t)$ is the estimated template for detecting $b[k]$ (as well as for future symbols, if needed). When past decisions are correct, $\hat{h}_k(t)$ approaches the optimal $\hat{h}(t)$ in (6) asymptotically as $k \to \infty$. The estimator in (7) does not require training overhead except during the initialization phase. A receiver using $\hat{h}(t)$ or $\hat{h}_k(t)$ as the correlation template is an autocorrelator, because the template is self-derived from the received signal $r(t)$.

An autocorrelation receiver can be viewed as a linear filter system that produces the symbol decision statistic $y[k]$ from the input waveform $r(t)$ via a filter $w(t) = \hat{h}(t)$. A binary decision can then be made according to $\hat{b}[k] = \text{sgn}\{y[k]\}$. It is thus natural to make connections with filter theory which may benefit our algorithm development and analysis. Let $x \cdot y := \int_0^{T_b} x(t)y(t)dt$ denote the inner product of two time-functions $x(t)$ and $y(t)$. Meanwhile, let $||x||^2 := \int_0^{T_b} x^2(t)dt$. Treating $w_k(t) = \hat{h}_k(t)$ as an adaptive filter, the following basic relations arise [15]:

filter output:	$y[k] = \int_0^{T_b} w_k(t)r_k(t)dt = w_k \cdot r_k$
desired output:	$d[k] = b[k]$
estimation error:	$e[k] = d[k] - y[k]$
decision direction:	$d[k] = \text{sgn}\{y[k]\}$.

Because of the decision direction $d[k] = \hat{b}[k]$ involved, we term the overall detector a decision directed autocorrelation (DDA) filter. The problem of estimating the correlation template $w(t)$ boils down to updating the adaptive filter weight $w_k(t)$. Implementation of the DDA detector in (7) can be accomplished either in batch operation or in an iterative manner. The former has faster convergence at the expense of higher complexity, while the latter is simpler to implement with an extra benefit of being capable of adapting to slow time-varying channels. Several implementation options will be presented next.

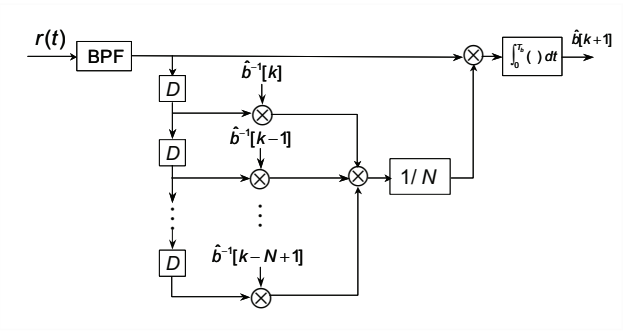

Fig. 1. Sliding-window based DDA receiver.

A. Sliding-Window Based DDA Detector

To implement (7) with a fixed filter memory length, we consider a sliding window approach in which the correlation-template filter $w_k(t)$ for detecting the k-th symbol is derived from the received symbol waveforms and the corresponding data decisions within a window of N symbol intervals preceding the current symbol. Specifically, $w_k(t)$ is constructed as

$$w_k(t) = \frac{1}{N}\sum_{j=1}^{N}\hat{b}[k-j]r_{k-j}(t). \tag{8}$$

This sliding-window DDA receiver is illustrated in Fig. 1. The data-demodulated (using symbol decisions) received signal from bits $k-N$ to $k-1$ are delayed and summed in an analog fashion. For initialization, a group of N pilot symbols are used at the beginning of the transmission to generate the initial template waveform and symbol decisions. Afterwards, the receiver is switched to the DD mode without using any pilot symbol.

In (8), the signal component of $w_k(t)$ is given by $\gamma_k\sqrt{E_b}h(t)$, which is exactly the ideal channel subject to scaling by $\sqrt{E_b}$ and an estimation efficiency factor $\gamma_k = \frac{1}{N}\sum_{j=1}^{N} b[k-j]\hat{b}[k-j]$ in the range of $[0,1]$. When feedback decisions are correct, it holds that $\hat{b}[k-j] = b[k-j]$, $\forall k$, and $\gamma_k = 1$, which corresponds to maximum estimation efficiency equivalent to the training case. The correlation template can be equivalently written as

$$w_k(t) = \gamma_k\sqrt{E_b}h(t) + \xi_k(t). \tag{9}$$

where $\xi_k(t) = \frac{1}{N}\sum_{j=1}^{N}\hat{b}[k-j]n_{k-j}(t)$ is the noise component of the self-derived template. It can be shown that the PSD of $\xi_k(t)$ is $\sigma_k^2(N_o/2)$ with $\sigma_k^2 = 1/N$, $\forall k$. Obviously, $w_k(t)$ is very close to the optimal correlation template when N is large, as long as the channel remains static within the N symbol periods.

B. Recursive DDA Detector

The sliding window DDA detector requires N analog delay units, which can be expensive when N is large. To

TABLE I
DECISION DIRECTED AUTOCORRELATION RECEIVERS

Initialization	$w_1(t) = (1/N)\sum_{n=-(N-1)}^{0} b[n]r_n(t)$, with training bits $\{b[1-N], \ldots, b[0]\}$ known.
Filter output	$y[k] = w_k \cdot r_k$
Bit decision	$\hat{b}[k] = \text{sgn}\{y[k]\}$
Weight updating	sliding-window DDA: $w_{k+1}(t) = \frac{1}{N}\sum_{i=0}^{N-1} \hat{b}[k-i]r_{k-i}(t)$ recursive DDA: $w_{k+1}(t) = \mu w_k(t) + \hat{b}[k]r_k(t)$ LMS DDA: $w_{k+1}(t) = w_k(t) + \alpha r_k(t)(\hat{b}[k] - y[k])$

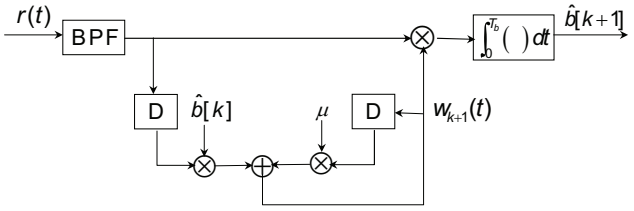

Fig. 2. Low-complexity recursive decision directed autocorrelation structure.

reduce hardware complexity, next we implement (7) in a recursive manner, where an update yielding the new template $w_{k+1}(t)$ relies only on the current template $w_k(t)$ and the newly received waveform $r_k(t)$. Common in adaptive filter designs, an alternative to (7) is given by the weighted time average $w_k(t) = \sum_{i=0}^{k-1} \mu^{k-1-i}\hat{b}[i]r_i(t)$, where μ is a positive exponential forgetting factor less than 1. This factor allows the template filter to accommodate possible non-stationarities in the input and gives adaptation capability in the presence of time-varying fading. In an iterative manner, the weighted-average expression leads to the following template estimate for a recursive DDA detector:

$$w_{k+1}(t) = \mu w_k(t) + \hat{b}[k]r_k(t). \tag{10}$$

The overall receiver structure is shown in Fig. 2, which only requires two delay units. Similar to (9), we can express the template estimate as $w_k(t) = \gamma_k\sqrt{E_b}h(t) + \xi_k(t)$. Here γ_k is given by $\gamma_k = \sum_{i=0}^{k-1} \mu^{k-1-i}\hat{b}[i]b[i]$ which reduces to $\gamma_k = (1-\mu^k)/(1-\mu)$ under accurate past decisions. The noise PSD is given by $\sigma_k^2(N_o/2)$ with $\sigma_k^2 = (1-\mu^{2k})/(1-\mu^2)$.

C. LMS Based DDA Detector

In Sections III-A and III-B, decision direction is adopted to replace training symbols in the process of channel estimation. Alternatively, we may utilize decision direction as indication of the quality of past waveforms, which will in turn determine how these waveforms contribute to the updated correlation template. The goal is to detect $b[k]$ rather than estimating $h(t)$ per se. Next we present a least mean square (LMS) filter that provides a simple implementation of such an approach.

Consider the following least-square formulation for designing the template $w_k(t)$:

$$\min_{w_k} \; J(k) = \sum_{i=0}^{k} e^2[k] = \sum_{i=0}^{k} |d[k] - w_k \cdot r_k|^2 . \tag{11}$$

In the DD mode, the LMS solution to (11) yields the following adaptation steps:

$$\hat{b}[k] = \text{sgn}\{w_k \cdot r_k\} \tag{12a}$$
$$e[k] = \hat{b}[k] - w_k \cdot r_k \tag{12b}$$
$$w_{k+1}(t) = w_k(t) + \alpha r_k(t)e[k] \tag{12c}$$

where α is the step size taking on a small value. Considering the fluctuation in the instantaneous received energy $||r_k||^2 := \int_0^{T_b} r_k^2(t)dt$, we may set $\alpha = \tilde{\alpha}/||r_k||^2$ or $\alpha = \tilde{\alpha}/(a + ||r_k||^2)$ with constants $a > 0$ and $0 < \tilde{\alpha} < 2$. These choices give rise to the normalized LMS algorithm, which is convergent in the mean square and potentially converges faster than a standard LMS algorithm [15].

To implement (12c), the same receiver structure in Fig. 2 applies. However, the input $r_k(t)$ in (12c) is not demodulated by $\hat{b}[k]$ before being added to the new filter update $w_{k+1}(t)$. Instead, it is adjusted by $\hat{b}[k]$ via the filter estimation error $e[k]$, which depends on the projected difference between $\hat{b}[k]$ and $r_k(t)$ rather than their cross-correlation as in (10). This operation reflects a different mechanism from that used in (8) and (10). In fact, LMS-based DDA filter corresponds to an adaptive implementation of the optimal Wiener filter $w_o(t) = arg\min \text{E}\{|b[i] - w_o \cdot r_i|^2\}$, whereas recursive DDA filter corresponds to an optimal matched filter $h(t)$. The template estimate in the LMS DDA filter can still be subsumed by $w_k(t) = \gamma_k^{(LMS)}\sqrt{E_b}h(t) + \xi_k^{(LMS)}(t)$, except that the noise term $\xi_k^{(LMS)}(t)$ has non-zero mean due to the bias between $w_o(t)$ and $h(t)$.

D. Implementations

All these DDA filters rely on decision direction, in which case initialization becomes an imminent issue. Similar to conventional DD methods, initialization is typically accomplished via training or other sub-optimal low-complexity processing. A training based initialization method has been discussed in Section III-A, which can be used for other DDA algorithms as well. The adaptive procedures for all three DDA receivers are summarized in Table I.

Among the three DDA receivers, sliding-window DDA has the highest implementation complexity in terms of the number of delay units required. The other two iterative filters have similar hardware complexity, while LMS-based DDA has slightly higher computational load than recursive DDA.

Compared with other UWB receivers, all of the proposed autocorrelators build upon analog or digital delay-and-average units operating at the *symbol rate*. Asymptotically optimal

correlation templates capable of sufficient energy capture are constructed without explicit channel estimation and multipath tracking of path gains and delays, nor do they require pilot symbol overhead. In contrast, implementing a proper correlation template for a RAKE receiver rely on digital operations at an impractical *sub-pulse rate*, as well as computationally-involved estimation of channel state information.

IV. Performance Analysis

In this section, we analyze the proposed adaptive DDA UWB receivers in terms of their steady-state BER performances and algorithm convergence rates. We will first assume that all past decisions are accurate. Such analysis is common for DD methods, and establishes tangible bounds for benchmarking performance in the high SNR region. BER performance in the low SNR region will also be discussed to take into account the effect of incorrect past decisions.

A. Convergence

Under accurate past decisions, both sliding-window and recursive DDA filters can be written in a unifying form after normalization, as follows:

$$w_k(t) = \sqrt{E_b}h(t) + \sigma_\xi[k]\bar{\xi}(t), \tag{13}$$

where $\bar{\xi}(t) = \xi_k(t)/\sigma_k$ is the normalized noise term with a fixed PSD $N_o/2$, and $\sigma_\xi[k] = \sigma_k/\gamma_k$. The two filters differ only in $\sigma_\xi^2[k]$, which is given by

$$\sigma_\xi^2[k] = \begin{cases} \dfrac{1}{N}, & \text{sliding-window DDA;} \\ \dfrac{1+\mu^k}{1-\mu^k}\dfrac{1-\mu}{1+\mu}, & \text{recursive DDA.} \end{cases} \tag{14}$$

For the adaptive filter in (13), its rate of convergence can be evaluated by $\sigma_\epsilon^2[k] := \mathrm{E}\{\epsilon_k^2\}$, which is the mean square value of the filter estimation error $\epsilon_k(t) := w_k(t) - \sqrt{E_b}h(t)$. It is straightforward to show that

$$\sigma_\epsilon^2[k] = \sigma_\xi^2[k](N_o/2)BT_b, \qquad \text{when } 1/B \le T_b. \tag{15}$$

Based on (14), it is apparent that sliding-window DDA has a fixed error variance across k, which is determined by the sliding window size N. In contrast, the error variance of recursive DDA drops as k increases, and has a convergence rate of $1/k$ when $\mu = 1$. At the steady state, the filter error variance is proportional to $\tilde{\sigma}_\xi^2 := \lim_{k\to\infty} \mathrm{E}\{\sigma_\xi^2[k]\}$, which equals $1/N$ for sliding-window DDA and $(1-\mu)/(1+\mu)$ for recursive DDA, provided that the channel is time invariant.

It is also possible to analyze the rate of convergence of the LMS DDA filter, and possibly its tracking capability in the presence of time-varying channels [15]. Unfortunately, there is no proper time-varying model for UWB propagation channels, which leaves this topic for future exploration.

B. BER Performance

To analyze the steady-state BER performance of the proposed adaptive receivers in UWB fading channels, we will use a practical channel model whose structure and parameters are explained in Section II. To provide a general result, we allow the time-window of the correlator to have a flexible length $T_L \le T_b$, which corresponds to collecting the first arrived L_p ($L_p \le L$) paths. Correlating the filtered signal waveform $r(t)$ with the self-derived template waveform $w_k(t)$ in (13), the decision variable for the k^{th} bit is obtained as

$$y[k] = \int_{iT_b}^{iT_b+T_L} r_k(t)w_k(t)dt = b[k]\theta + z_1 + z_2 + z_3, \tag{16}$$

where the first term $b[k]\theta$ in (16) is the desired signal term, while z_1, z_2 and z_3 are noise terms, given respectively by

$$\theta = E_b \int_{iT_b}^{iT_b+T_L} h^2(t)dt, \tag{17a}$$

$$z_1 = \sqrt{E_b}\tilde{\sigma}_\xi \int_{iT_b}^{iT_b+T_L} h(t)\bar{\xi}(t)dt, \tag{17b}$$

$$z_2 = \sqrt{E_b} \int_{iT_b}^{iT_b+T_L} h(t)n(t)dt, \tag{17c}$$

$$z_3 = \tilde{\sigma}_\xi \int_{iT_b}^{iT_b+T_L} n(t)\bar{\xi}(t)dt. \tag{17d}$$

In order to determine the analytical BER expression for binary PAM signals, we will derive the conditional BER from (16) depending on a given realization of the random channel coefficients $\boldsymbol{\alpha} = \{\alpha_0, \cdots, \alpha_{L_p-1}\}$. This instantaneous performance will then be integrated over the joint probability density function (pdf) of the random parameters to obtain the average BER.

1) Distribution of $z_1 + z_2 + z_3$: Evaluation of the distribution of the composite noise $z = z_1 + z_2 + z_3$ has been shown to be a complex procedure [7], [16], [17]. The DPSK performance analysis in [16], [17] is not applicable to the new characteristics in this DDA receiver. The performance evaluation in [7] analyzed a very similar scenario as that of this DDA receiver. However, it did not give an easy-to-use solution and its calculation complexity is high. Here we derive a BER expression which can approximately predict the performance reliably while keeping the complexity reasonable.

Because both $\bar{\xi}(t)$ and $n(t)$ are zero-mean Gaussian random processes independent of $h(t)$, the noise terms z_1 and z_2 can be regarded as zero-mean Gaussian random variables. When BT_b is large, the noise product term z_3 can also be well approximated as a Gaussian random variable for SNR regions of practical interest [6], [7], [16], [17]. The mean value of z_3 is zero when the bandwidth B is an integer of $1/(2T_b)$, as we have assumed in Section II. By using $R_n(T_b) = 0$, it is straightforward to show that all three noise terms are uncorrelated, i.e., $E\{z_1z_2\} = E\{z_1z_3\} = E\{z_2z_3\} = 0$ [6], [7], [16], [17].

By using (4) and (17), and employing the assumption $B \gg 1/T_L$, the noise variance can be approximately evaluated as [16], [17]

$$\sigma_z^2 \cong \theta\frac{N_o}{2}(1+\tilde{\sigma}_\xi^2) + BT_L\tilde{\sigma}_\xi^2 N_o^2. \tag{18}$$

2) Distribution of θ: Let $R_h(\tau) := \int_0^\tau h^2(t)dt$ denote the channel energy as a function of the integration window length τ. From (17a), the effective sample gain θ is given by $\theta = E_bR_h(T_L)$. Focusing on the UWB indoor channel model in [5], we suppose for analytical clarity that all channel paths arrive separately in time, i.e., there is no pulse overlapping.

Under this assumption, the received sample gain θ can be simplified to $\theta = \sum_{l=0}^{L_p-1} E_b \alpha_l^2$. Apparently, it is the sum of squared multipath fading coefficients, which are independent lognormal random variables (RVs). To evaluate the pdf of θ, one needs to find the pdf of a sum of independent lognormal RVs. Although an exact closed-form expression does not exist, there are a number of methods to approximate this pdf. We will apply the Wilkinson's method [18] to approximate the desired pdf of θ.

As mentioned in Section II, the channel coefficient α_l can be modeled as $\alpha_l = \lambda_l \beta_l$, where $\lambda_l \in \{1, -1\}$ and $\beta_l = |\alpha_l|$ is a lognormal RV. Let $\beta_l := |\alpha_l| = e^{u_l}$, where u_l is a normal RV obeying $u_l \sim \mathcal{N}(\mu_{u_l}, \sigma_{u_l}^2)$, and $\theta_l := E_b \alpha_l^2 = e^{c_0 + 2u_l}$, where $c_0 = \ln(E_b)$. The k^{th} moment of the lognormal variable β_l is then given by

$$E\{\beta_l^k\} = e^{k\mu_{u_l} + k^2\sigma_{u_l}^2/2}. \tag{19}$$

According to Wilkinson's method, we let $\theta = \sum_{l=0}^{L_p-1} \theta_l$ be modeled as a lognormal RV, that is, $\theta = e^x$ where $x \sim \mathcal{N}(\mu_x, \sigma_x^2)$ is a normal RV. The two parameters μ_x and σ_x can be obtained by matching the first two moments of θ with the first two moments of $\sum_{l=0}^{L_p-1} \theta_l$. Algebraic manipulations lead to the mean $\mu_x = \ln(E_{L1}^2/\sqrt{E_{L2}})$ and the variance $\sigma_x = \sqrt{\ln(E_{L2}/E_{L1}^2)}$, where the two scalars E_{L1} and E_{L2} are related to μ_{u_l} and $\sigma_{u_l}^2$ by

$$E_{L1} = \sum_{l=0}^{L_p-1} e^{(c_0 + 2\mu_{u_l} + 2\sigma_{u_l}^2)} \tag{20a}$$

$$E_{L2} = \sum_{l=0}^{L_p-1} e^{2(c_0 + 2\mu_{u_l} + 4\sigma_{u_l}^2)} + 2\sum_{l=1}^{L_p-1}\sum_{m=0}^{l-1} e^{2(c_0 + \mu_{u_l} + \mu_{u_m} + \sigma_{u_l}^2 + \sigma_{u_m}^2)}. \tag{20b}$$

Putting all together, the pdf of θ is approximated as

$$f(\theta) = \frac{1}{\theta\sqrt{2\pi\sigma_x^2}} exp\left[-\frac{(\ln(\theta) - \mu_x)^2}{2\sigma_x^2}\right]. \tag{21}$$

3) Error Performance: Conditioned on θ, the BER expression of a binary PAM signal is given by

$$P(\theta) = \frac{1}{\sqrt{2\pi\sigma_z^2}} \int_{-\infty}^{0} exp\left[-\frac{(\lambda - \theta)^2}{2\sigma_z^2}\right] d\lambda = Q\left(\frac{\theta}{\sigma_z}\right) \tag{22}$$

where $Q(\cdot)$ is the complementary error function.

The average BER can be calculated by averaging the conditional BER $P(\theta)$ over the probability density function $f(\theta)$ in (21) as

$$P_b = \int_0^\infty P(\theta) f(\theta) d\theta. \tag{23}$$

This BER expression applies to any channel type without necessarily incurring the assumption of no pulse overlapping. In a general case, the pdf $f(\theta)$ should be replaced by the actual channel statistic and can be evaluated via Monte Carlo simulations. Numerical methods can be used to evaluate the BER in (23), which provides the performance lower bound under the assumption of perfect past decisions.

C. Error Performance in Low SNR Region

Albeit fairly accurate at the high SNR region, the BER expression in (23) cannot precisely describe the receiver error performance for low SNRs, in which case the number of erroneous past decisions becomes non-trivial. Here we examine the low-SNR case to provide some insight on the receiver performance. Our approach relies on counting the probability of erroneous symbol decisions.

Recall the template estimate $w_k(t)$ in (8). When past decisions are in error, the noise term $\xi_k(t)$ in the template remains un-affected, but the estimation efficiency factor γ_k is lowered. Each wrong symbol decision will cause its corresponding waveform to counteract a correctly demodulated waveform. As a result, γ_k should be replaced by $\gamma_k' = (1 - 2P(\theta))\gamma_k$ to accommodate the effect of wrong decisions. It is reasonable to assume that $P(\theta)$ must be less than 50% for a meaningful transmission. Corresponding to (13), the low-SNR general expression for $w_k(t)$ can be written as

$$w_k(t) = (1 - 2P(\theta))\sqrt{E_b} h(t) + \sigma_\xi^2[k]\bar{\xi}(t). \tag{24}$$

The decision statistic $y[k]$ in (16) should be adjusted accordingly. The effective sample amplitude θ should be replaced by $\theta' = (1 - 2P(\theta))\theta$ and the second noise term in (17c) replaced by $z_2' = (1 - 2P(\theta))z_2$, while z_1 and z_3 remain the same. The composite noise variance is now $\sigma_z'^2 \cong \theta(1 - 2P(\theta) + \tilde{\sigma}_\xi^2)(N_o/2) + BT_L\tilde{\sigma}_\xi^2 N_o^2$. Substituting θ' and $\sigma_z'^2$ for θ and σ_z^2 in (22), we obtain an expression for $P(\theta)$ in the low SNR region:

$$P(\theta) = Q\left(\frac{\theta'}{\sigma_z'}\right) = Q\left(\frac{(1 - 2P(\theta))\theta}{\sqrt{\theta(1 - 2P(\theta) + \tilde{\sigma}_\xi^2)N_o/2 + BT_L\tilde{\sigma}_\xi^2 N_o^2}}\right). \tag{25}$$

Eq. (25) does not immediately lead to a manageable closed-form solution to $P(\theta)$. Nevertheless, some one-dimensional numerical methods may be used to find an approximate solution to $P(\theta)$ given θ. In next section, we compute the BER performance based on the numerical solution to (25) and compare it with both the analytical result in (22) and simulation results.

V. Numerical Results

In all simulation tests, we use the CM3 model from [5] to generate random UWB channel realizations. The root-mean-square (RMS) channel delay spread is set to 15ns, the average cluster arrival rate is 0.0667/ns, and the average path arrival rate is 2/ns. The cluster and ray decay factors are given by $\Gamma = 14$ns and $\gamma = 7.9$ns, respectively. The standard deviation of the fading coefficients is set to be 3.4dB. There are a total number of $L = 35$ resolvable paths, whose total energy is normalized by $E\{\sum_{l=0}^{L-1} |\alpha_l|^2\} = 1$. A carrier-modulated, truncated root-raised-cosine (RRC) pulse with a roll-off factor of 0.25 is applied as the UWB pulse shape $p(t)$ and the pulse width is set to $T_p = 0.5$ns. The transmission rate $1/T_b$ is selected to be such that channel excess delay does not cause ISI.

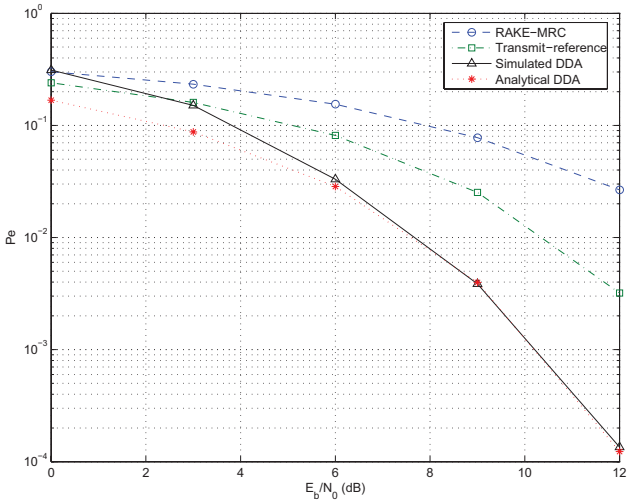

Fig. 3. Analytical and simulated BER versus average received SNR curves using different receiver schemes. L_p is 35 for DDA and TR, 5 for RAKE.

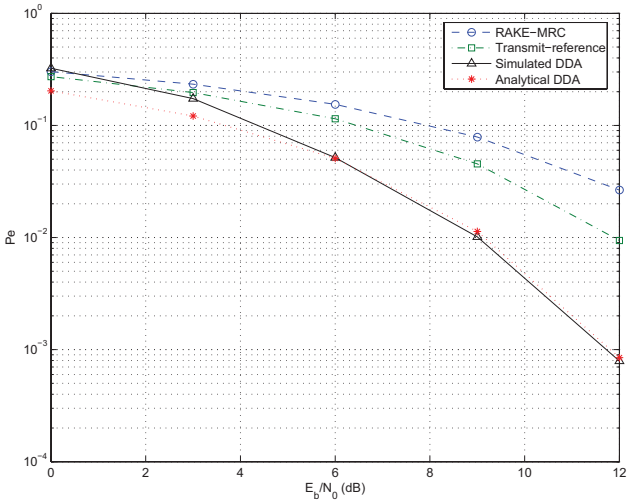

Fig. 4. BER versus SNR for various receiver schemes: L_p is 20 for DDA and TR, 5 for RAKE.

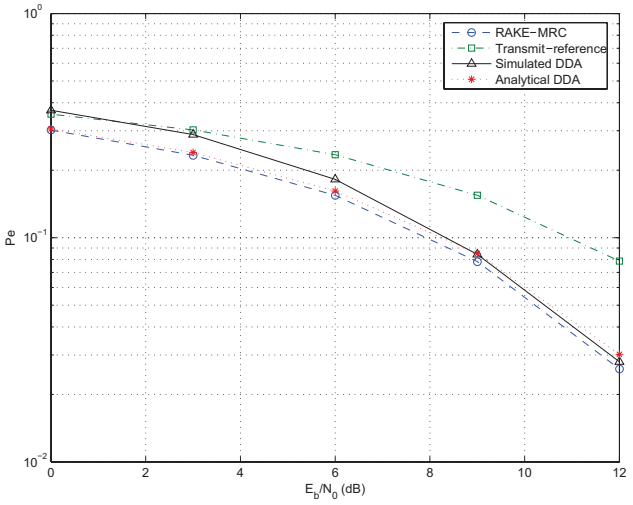

Fig. 5. BER versus SNR for various receiver schemes: L_p = 5 for all schemes.

Three different receivers are considered: the RAKE receiver with maximum ratio combining (MRC), the transmit-reference (TR) receiver, and the proposed sliding-window DDA receiver with a pilot symbol block of size $N = 16$ for initialization. The DDA receiver may use the signal waveform collected from all paths or just collect a part of the received signal energy from the first received L_p paths. In the RAKE receiver, the number of fingers is set to be 5, which is a reasonable limit imposed by practical receiver cost constraints.

The BER curves of these receivers are plotted in Figs. 3, 4, and 5, with $L_p = 35, 20$ and 5, respectively. Analytical BER curves of the DDA receiver are also included to compare with the simulated curves. In all test cases, the proposed DDA receiver performs better than the TR receiver. The analytical performance of the DDA receiver matches well with its simulated results in high SNR region, except in Fig. 5 where $L_p = 5$ is not large enough for the Wilkinson's method [18] to achieve an accurate approximation of the pdf $f(\theta)$. In the low SNR region, as discussed in Section IV-C, because the analysis did not take into account erroneous symbol decisions, the analytical BER in (22) is lower than the actual value. To accommodate the effect of erroneous symbol decisions in DD, the low-SNR BER expression in (25) is evaluated numerically to solve for $P(\theta)$, which is then used in (23) to reach the average BER. This low-SNR analytical BER matches well with simulations, as shown in Fig. 6.

Due to the noise term in the template waveform, the DDA receiver and the TR receiver perform worse than the RAKE receiver when the same number ($L_p = 5$) of paths are collected, as shown in Fig. 5. However, the performance gap between the DDA and the RAKE receiver is small in high SNR region, since the noise effect has been mitigated by the averaging operation in the DDA receiver. As more paths are collected by the receiver (Figs. 3-4), both DDA and TR receivers outperform the 5-finger RAKE receiver. Note that collecting a large number of signal paths in DDA and TR does not raise implementation costs, as one can simply adjust the correlation time-window length T_L.

DDA receivers collecting different numbers of received paths are compared via simulations in Fig. 7. Apparently a receiver collecting more paths offers better BER performance, but the improvement does not increase proportionally because paths arriving earlier typically contain higher energy on average. The memory depth of the DD operation also affects the receiver performance, which is illustrated in Fig. 8. As expected, a larger N leads to a more noticeable reduction in the noise level of the constructed correlation template, which in turn improves the detection performance. In the high SNR region, it is noted that the BER performance can be effectively improved by increasing the number of collected paths L_p, while the improvement diminishes as the memory length N increases.

The sliding-window DDA receiver is compared with recursive DDA and LMS DDA receivers in Fig. 9. The latter two receivers are simpler to implement, yet exhibit BER performances comparable to that of sliding-window DDA. When the forgetting factor μ is selected to be larger than $(N-1)/(N+1)$ (based on the filter error variance factor $\tilde{\sigma}_\xi^2$ in (14) at the steady state), the recursive DDA has an effective

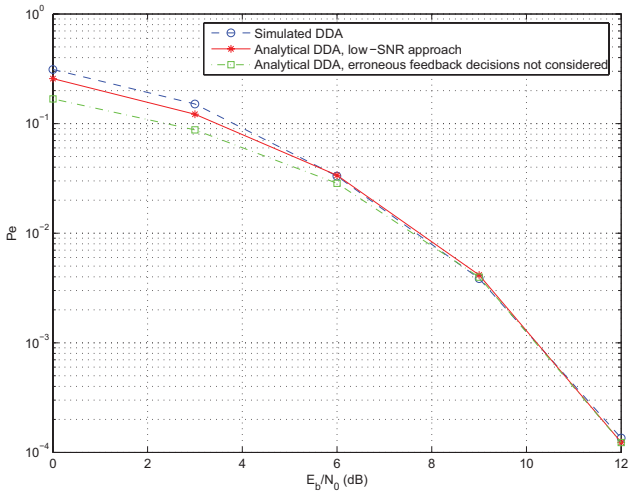

Fig. 6. BER versus SNR curves using the analytical approach given in Sections IV-B and IV-C: $L_p = 35$.

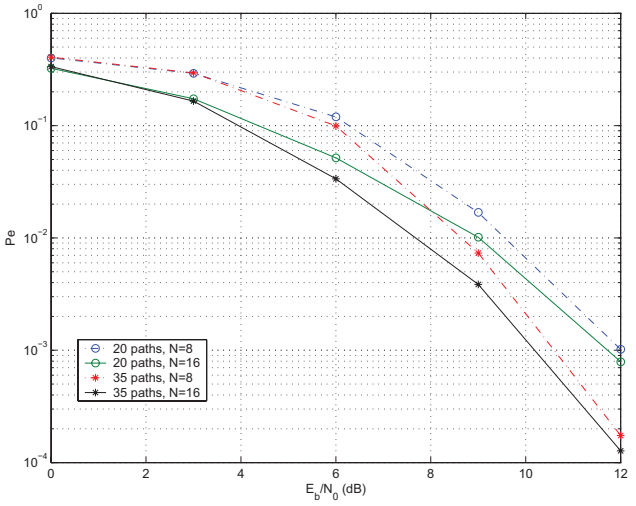

Fig. 8. Simulated BER curves for DDA receiver with different window length N.

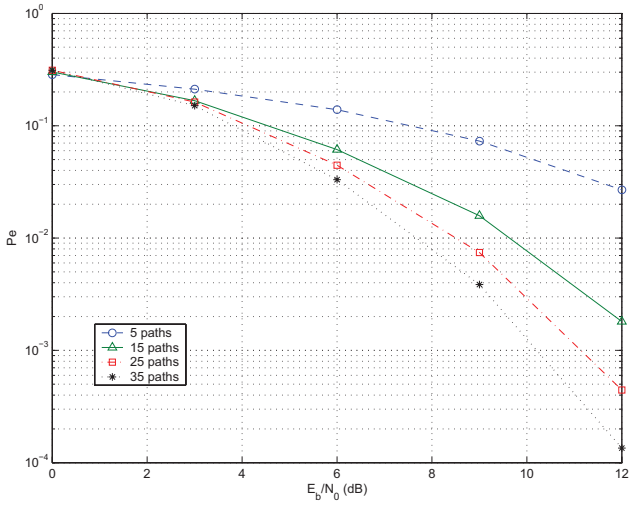

Fig. 7. Simulated BER curves for DDA receiver with different number of collected paths L_p

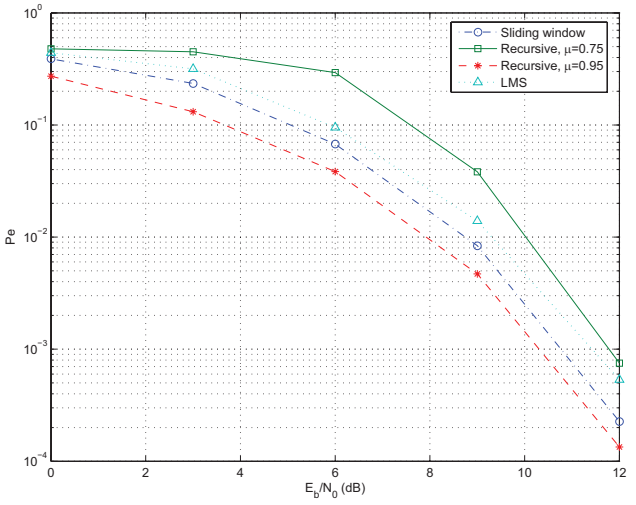

Fig. 9. Performance comparison among all three DDA schemes.

filter memory length longer than N, leading to better BER performance than sliding-window DDA at the steady state. In general, a larger μ leads to better steady state performance, but slower convergence. The LMS DDA receiver has slightly worse performance, because it is an adaptive implementation of Wiener filter, which does not take into account the finite-alphabet constraint on symbols $\mathbf{b}$.

The analysis and simulations so far have assumed a single-user communication scenario. The DDA receivers are expected to outperform TR schemes in multi-user scenarios as well, since the adaptive template-updating process can also mitigate the effect of multiple-access interference (MAI) on the quality of the template waveform. However, the exact performance of the DDA receiver in a multi-user scenario depends on many factors such as the spreading schemes (e.g., time-hopping, direct-sequence) and other system parameters. The analytical performance analysis of the proposed schemes in a multi-user environment is beyond the scope of this paper, and is thus left for further investigation. Instead, we provide simulation results to compare the DDA and the TR schemes in a multi-user scenario. Fig. 10 shows the BER versus the received signal-to-interference ratio (SIR) curves with different number of interferers. The bit rate is chosen to be 20Mbps and all other parameters are same as previous examples. In a multi-user environment, notwithstanding the error floor observed in both the DDA and the TR schemes, the performance advantage of DDA over TR is quite evident.

VI. Algorithm Enhancement via Soft Decoding

The detection performances of DDA receivers depend not only on the noise effect, but also on potential error propagation effect when past decisions are in error. For the latter, we employ a soft decoding strategy to mitigate the destructive effect of wrong decisions on the self-derived templates.

Recall the decision process for a binary PAM symbol. The decision statistic $y[k]$ is compared with the threshold 0 to make a hard decision $\hat{b}[k]$ on the corresponding symbol $b[k]$. Replacing $b[k]$ by the binary $\hat{b}[k]$ is termed *hard-decoding* based DDA. The instantaneous decision quality is determined by $|y[k]|$, which is the distance from the observation to the

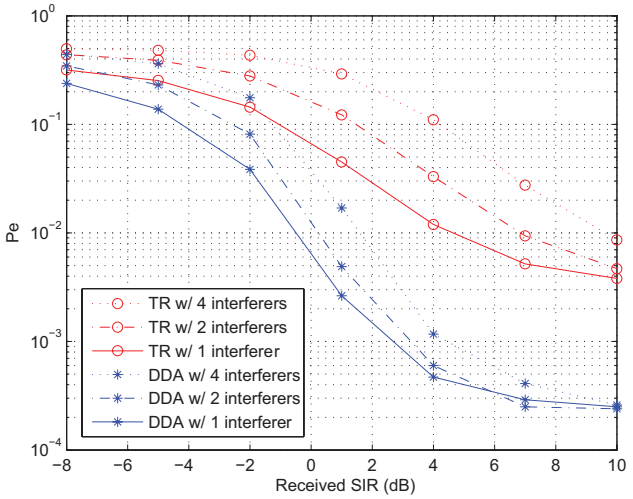

Fig. 10. Performance of DDA and TR receivers in multi-user scenarios: $E_b/N_0 = 12dB$.

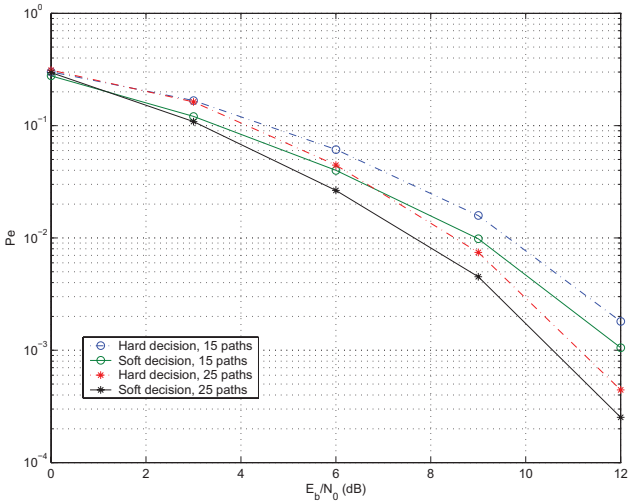

Fig. 11. Performance comparison between the hard decoding and soft decoding DDA schemes.

threshold, and is determined by the channel fading and noise experienced. When $|y[k]|$ is closer to 0, the detector is less confident about the decision, indicating a larger chance of making a detection error. However, in a hard-decision scheme, all past decisions affect the template estimate in the same manner, regardless of their different qualities indicated by $|y[k]|$. This degrades the estimation performance when wrong bit decisions occur.

To take advantage of the error detection capability provided by $|y[k]|$, we propose a *soft decoding* DDA scheme that is capable of reducing the impact of error-prone symbol decisions. Depending on the confidence level the detector has on a past decision, the contribution of this past symbol to the template estimate will be weighted. The smaller $|y[k]|$ is, the smaller its corresponding weight is. Based on this idea, we construct a weighting function $f(|y[k]|)$ that is monotonic in $|y[k]|$. A convenient choice is $f(x) = x$, which leads to a soft-decoding based DDA in the form of

$$w_k(t) = \frac{1}{k}\sum_{i=0}^{k-1} f(|y[i]|)\hat{b}[i]r_i(t) = \frac{1}{k}\sum_{i=0}^{k-1} y[i]r_i(t). \qquad (26)$$

Because the hard decision $\hat{b}[i]$ is replaced by non-quantized correlator output $y[i]$, a strong and clean symbol waveform will contribute more to the self-derived template waveform than a weak and noisy waveform. Other choices for $f(\cdot)$ are also possible. When $f(x) = 1$, $\forall x$, the weighting function is irrespective of the decision quality, and (26) reduces to the hard-decision scheme.

Sliding-window based soft-decoding DDA is compared with its hard-decision counterpart in Fig. 11, where the channel environment and transmission parameters are the same as those in Section V. A SNR advantage of $0.5 \sim 1$ dB is achieved by employing soft decoding.

VII. Conclusion

Decision-directed autocorrelation receivers are proposed and analyzed for pulsed UWB systems. The advantages and disadvantages of different implementations of the DDA scheme are analyzed and compared. The DDA schemes are simple to implement using delay and average units, and incur little training overhead for channel estimation. They are more effective in capturing multipath energy than practical RAKE receivers, and effectively improve the power efficiency and suppress the noise enhancement effect in the correlation template compared with TR receivers. The detection performance is further improved by a soft decoding approach that takes advantage of the error quality indicator provided by correlator outputs. Confirmed by both analytical error performances and simulation results, the DDA receivers outperform other alternatives, especially in the high SNR region.

References

[1] M. Z. Win and R. A. Scholtz, "Impulse radio: How it works," *IEEE Commun. Lett.*, vol. 2, pp. 36-38, Feb. 1998.

[2] J. Foerster, E. Green, V. S. Somayazulu, and D. Leeper, "Ultra-wideband technology for short- or medium-range wireless communications," *Intel Technology Journal*, Q2, 2001.

[3] M. Z. Win and R. A. Scholtz, "On the energy capture of ultrawide bandwidth signals in dense multipath environments," *IEEE Commun. Lett.*, vol. 2, no. 9, pp. 245-247, Sep. 1998.

[4] S. Gaur and A. Annamalai, "Improving the range of UWB transmission using RAKE receivers," in *Proc. 53rd IEEE VTC*, vol. 1, pp. 597-601, Oct. 2003.

[5] A. F. Molisch, J. R. Foerster, and M. Pendergrass, "Channel models for ultrawideband personal area networks," *IEEE Wireless Commun.*, vol. 10, no. 6, pp. 14-21, Dec. 2003.

[6] R. T. Hoctor and H. W. Tomlinson, "An overview of delay-hopped, transmitted-reference RF communications," *Technical Information Series*, G.E. Research and Development Center, pp. 1-29, Jan. 2002.

[7] J. D. Choi and W. E. Stark, "Performance of ultra-wideband communications with suboptimal receiver in multipath channels," *IEEE J. Select. Areas Commun.*, vol. 20, no. 9, pp. 1754-1766, Dec. 2002.

[8] L. Yang and G. B. Giannakis, "Optimal pilot waveform assisted modulation for ultra-wideband communications," *IEEE Trans. Wireless Commun.*, vol. 3, no. 4, pp. 1236-1249, July 2004.

[9] H. Zhang and D. L. Goeckel, "Generalized transmitted-reference UWB systems," in *Proc. IEEE UWBST*, Nov. 2003, pp. 147-151.

[10] A. Trindade, Q. H. Dang, and A. van der Veen, "Signal processing model for a transmit-reference UWB wireless communication system," in *Proc. IEEE UWBST*, Nov. 2003, pp. 270-274.

[11] G. Leus, and A. van der Veen, "Noise suppression in UWB transmitted reference systems," in *Proc. Signal Processing Advances in Wireless Communications*, July 2004, pp. 155-159.

[12] Y.-L. Chao and R. Scholtz, "Optimal and suboptimal receivers for ultra-wideband transmitted reference systems," in *Proc. IEEE Glboecom*, Dec. 2003, pp. 759-763.
[13] G. Durisi and S. Benedetto, "Performance of coherent and non-coherent receivers for UWB communications," in *Proc. IEEE ICC*, pp. 3429-3433, June 2004.
[14] S. Zhao, H. Liu, and Z. Tian, "A decision-feedback authcorrelation receiver for pulsed ultra-wideband systems," in *Proc. IEEE Radio and Wireless Conference*, Sep. 2004, pp. 251-254.
[15] S. Haykin, *Adaptive Filter Theory*. Upper Saddle River, NJ: Prentice Hall, 1996.
[16] M. K. Simon, S. M. Hinedi, and W. C. Lindsey, *Digital Communication Techniques*. Englewood Cliffs, NJ: Prentice Hall, 1995.
[17] J. H. Park, "On binary DPSK detection," *IEEE Trans. Commun.*, vol. 26, pp. 484-486, Apr. 1978.
[18] N. C. Beaulieu, A. A. Abu-Dayya, and P. J. Mclane, "Estimating the distribution of a sum of independent lognormal random variable," *IEEE Trans. Commun.*, vol. 43, pp. 2869-2873, Dec. 1995.

Shiwei Zhao (S'02) received his bachelor degree in computer science from the University of Science and Technology of China (USTC) in 1999. He is currently working toward the Ph.D. degree in wireless communications at the School of EECS, Oregon State University. He is doing research on the design and performance analysis of wireless communication systems, with specific focus on ultra-wideband (UWB) technologies. From Jan. 2005 to June 2005, he had an internship at Mitsubishi Electric Research Lab (MERL), where he worked on proposal drafting to IEEE 802.15.4a study group (low rate UWB systems). He has published some journal and conference papers and filed two patent applications.

Huaping Liu (S'95-M'97) received his B.S. and M.S. degrees from Nanjing University of Posts and Telecommunications, Nanjing, P.R. China, in 1987 and 1990, respectively, and his Ph.D. degree from New Jersey Institute of Technology, Newark, NJ, in 1997, all in electrical engineering. From July 1997 to August 2001, he was with Lucent Technologies, New Jersey. Since September 2001, he has been an assistant professor with the School of Electrical Engineering and Computer Science at Oregon State University. His research interests include capacity and performance analysis of wireless systems, communication techniques for multiuser time-varying environments with applications to cellular and indoor wireless communications, ultra-wideband schemes, and MIMO OFDM systems.

Zhi Tian (M'98) received the B.E. degree in Electrical Engineering (Automation) from the University of Science and Technology of China, Hefei, China, in 1994, the M. S. and Ph.D. degrees from George Mason University, Fairfax, VA, in 1998 and 2000. From 1995 to 2000, she was a graduate research assistant in the Center of Excellence in Command, Control, Communications and Intelligence (C3I) of George Mason University. Since August 2000, she has been with the department of Electrical and Computer Engineering, Michigan Technological University, where she is currently an Associate Professor. Her current research focuses on signal processing for wireless communications, particularly on ultra-wideband systems. Dr. Tian serves as an Associate Editor for IEEE TRANSACTIONS ON WIRELESS COMMUNICATIONS. She is the recipient of a 2003 NSF CAREER award.